Proton structure from multiparticle contribution to elastic pp-scattering at 7 TeV

I.M. Dremin

Lebedev Physical Institute, Moscow 119991, Russia

The parton content of protons gets strong peripheral contribution at 1 fm from multiparticle dynamics as revealed by the overlap function in the unitarity condition for elastic pp-scattering at 7 TeV.

It is well known that parton (quark, gluon) densities and the share of low-x partons rise with increasing energies of colliding hadrons. Less attention has been paid to the analysis of the spatial distribution of the parton content inside them and its evolution with energy. This can be done by studying the structure of the overlap function in the unitarity condition for the elastic scattering amplitude in the impact parameter representation at different energies of colliding protons. The very first analyses [1, 2, 3] have lead to extremely interesting conclusions about the increasing peripherality of protons within the rather narrow interval of ISR energies. Later, this was confirmed and strengthened at somewhat higher energies by the S$p\bar{p}$S data [4]. It was shown that while the increase of the overlap function at the proton periphery is quite modest in the ISR energy range (about 4%), it becomes much stronger (about 12%) if S$p\bar{p}$S energies are included. However, no sizable change of the proton blackness was noticed at small distances in this energy interval. The similar effect at HERA energies was discussed in [5] for the vector meson production process in the framework of the dipole-proton scattering model.

That is why we attempt to learn if peripheral regions of protons become even more active at LHC energies and the central region is activated as well. The striking, but not at all unexpected, result is that this increase persists and extends to smaller impact parameters now. It amounts to about 40% of edge corrections at distances about 1 fm. The main parton content in the overall region of inelastic collisions remains relatively constant and below the unitarity bound in the central region of impact parameters less than about 0.5 fm but also indicates some increase of opacity compared to lower energies.

We proceed by using the approach adopted in [3]. First of all, the TOTEM data on the differential cross section of elastic pp-scattering at 7

TeV [6] are fitted by the formula (1) for the elastic scattering amplitude $f(s,t)$ (which depends on the center-of-mass energy $\sqrt{s}$ and the transferred momentum $\sqrt{|t|}$) proposed in [7]:

$$f(s,t) = i\alpha[A_1 \exp(0.5b_1\alpha t) + A_2 \exp(0.5b_2\alpha t)] - iA_3 \exp(0.5b_3 t), \qquad (1)$$

where $\alpha(s)$ is complex and is given by

$$\alpha(s) = [\sigma_t(s)/\sigma_t(23.5\text{GeV})](1 - i\rho_0(s)). \qquad (2)$$

Even though this parametrization has no theoretical foundation, it provides in a wide energy interval good phenomenological fits of differential cross sections[1] defined as

$$\frac{d\sigma}{dt} = |f(s,t)|^2. \qquad (3)$$

The normalization at the optical point is

$$\sigma_t(s) = \sqrt{16\pi}\text{Im}f(s,0). \qquad (4)$$

We shall also use the ratio of the real to imaginary parts of the amplitude

$$\rho(s,t) = \frac{\text{Re}f(s,t)}{\text{Im}f(s,t)}. \qquad (5)$$

The following values of the parameters have been fixed by the fit to the experimental points of the differential cross section at the energy 7 TeV in the range $0.0052 < |t| < 2.44$ GeV^2:

$$A_1^2 = 55.09\text{mb/GeV}^2, \quad A_2^2 = 3.46\text{mb/GeV}^2, \quad A_3^2 = 1.47\text{mb/GeV}^2,$$
$$b_1 = 8.31\text{GeV}^{-2}, \quad b_2 = 4.58\text{GeV}^{-2}, \quad b_3 = 4.70\text{GeV}^{-2}. \qquad (6)$$

We have also used $\sigma_t(7\text{ TeV}) = 98.58$ mb and $\rho_0(7\text{ TeV}) = 0.14$. The normalization of $|f(s,t)|^2$ in mb/GeV^2 allows direct comparison with [3].

The good quality of the fit with these values is seen in Fig. 1. With some adjustment of parameters A_i, b_i, the fit is also satisfactory if one adopts the value of $\rho_0 = 0.107$ favored by the recent results of the TOTEM collaboration [13].

The real and imaginary parts of the amplitude are shown in Fig. 2. Each of them has one zero. The evolution of their ratio $\rho(s,t)$ with the transferred momentum t is mainly prescribed by the last term in this formula with the negative sign in front of it and small exponential b_3. It is also shown in Fig. 2. It is small and can be neglected everywhere except near the point where the imaginary part is equal to zero.

[1] There are many others (albeit with larger number of adjustable and hidden parameters) reviewed in [8] and recently published [9, 10, 11, 12].

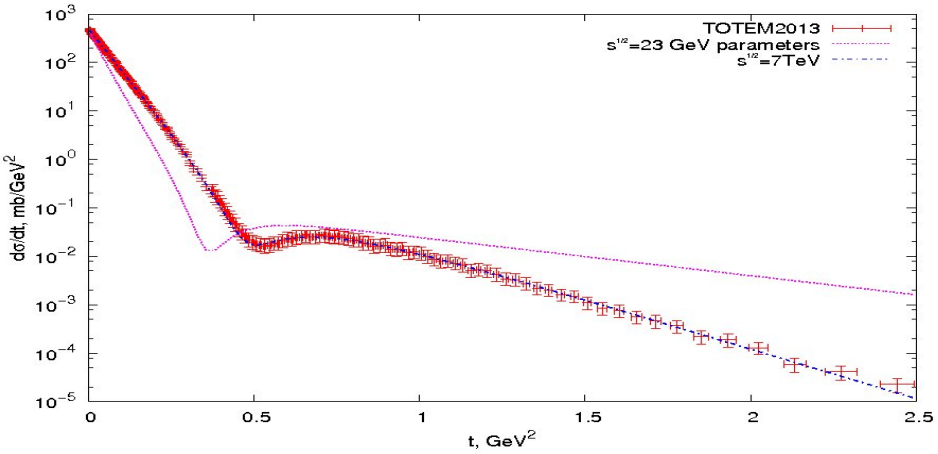

Fig. 1. Fit of the TOTEM data – dash-dotted curve. Dotted curve is calculated with parameters from [3] and with $\rho_0 = 0.14$.

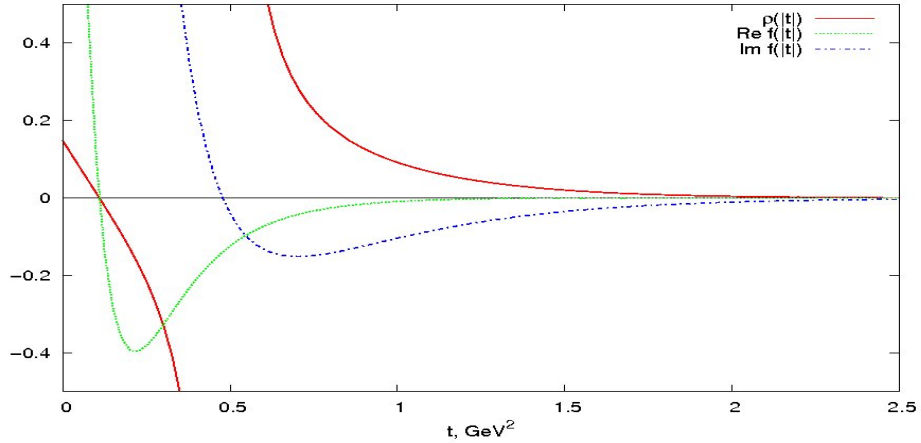

Fig. 2. Real (dotted curve) and imaginary (dash-dotted curve) parts of the amplitude and their ratio (solid curve).

The new feature seen in Fig. 2 is the difference in values of $\rho(s,t)$ in the Orear region for the two choices of ρ_0. It becomes of the order of 1 for $\rho_0 = 0.107$. Note that in both cases it strongly differs from its average value about -2 required by the fit according to the solution of the unitarity equation [14]. The solution [15] predicts the exponential of $\sqrt{|t|}$-behavior of the amplitude. It poses an interesting problem which has not yet been

resolved. This ratio can change the sign if more zeros of either imaginary or real parts of the amplitude appear. For example, this happens in the model of [11]. It incorporates phenomenologically the Orear type behavior of the amplitude at larger transferred momenta (albeit in a way somewhat different from [15]) and predicts two zeros of the real part. The ratio reaches large negative values at high transferred momenta. The somewhat smaller values at large $|t|$ are also predicted in the model using the inverse of polynomials [9] as described in [11]. The analysis of [11] clearly shows that the proper description of the amplitude at larger transferred momenta can change our conclusions about the behavior of this ratio there.

To reveal the space structure of proton interactions, the amplitude $f(s,t)$ must be rewritten in the impact parameter space. By applying the Fourier-Bessel transformation, we define the profile function

$$i\Gamma(s,b) = \frac{1}{\sqrt{\pi}} \int_0^\infty dqqf(s,t)J_0(qb). \tag{7}$$

Here, the variable b, called the impact parameter, describes the vector joining the centers of colliding protons at the moment of their collision, $q = \sqrt{-t}$, and J_0 is the Bessel function of zero order.

The amplitude $f(s,t)$ must satisfy the unitarity condition. If written in the impact parameter representation (7) it is

$$2\mathrm{Re}\Gamma(s,b) = |\Gamma(s,b)|^2 + G(s,b), \tag{8}$$

where G is called the overlap function in the impact parameter space.

The smallness of the real part of $f(t)$ corresponding to small $\mathrm{Im}\Gamma(s,b)$ implies that one can compute G approximately as

$$G(s,b) \approx 2\mathrm{Re}\Gamma(s,b) - (\mathrm{Re}\Gamma(s,b))^2. \tag{9}$$

The physics meaning of these relations is very simple. The overlap function G describes the kinematical overlap of two cones filled in by the inelastically produced secondary particles in the momentum space expressed in terms of the proton structure at a given impact parameter b. In other words, it corresponds to the particle distribution $d\sigma/db$ in the impact parameter space. One may treat it as a parton distribution if one-to-one correspondence of particles and partons is assumed.

The overlap function at 7 TeV has a form shown in Fig. 3 by the upper dash-dotted curve. Its dependence on $\rho(s,0)$ is so weak that can be neglected. However, as we see, it strongly differs from the corresponding function at ISR energy 23.5 GeV (shown by the lower solid curve), especially at the very edge of the distribution. The overlap function at 7 TeV declines steeply but there is no sharp cutoff at large impact parameters. At $b = 0$,

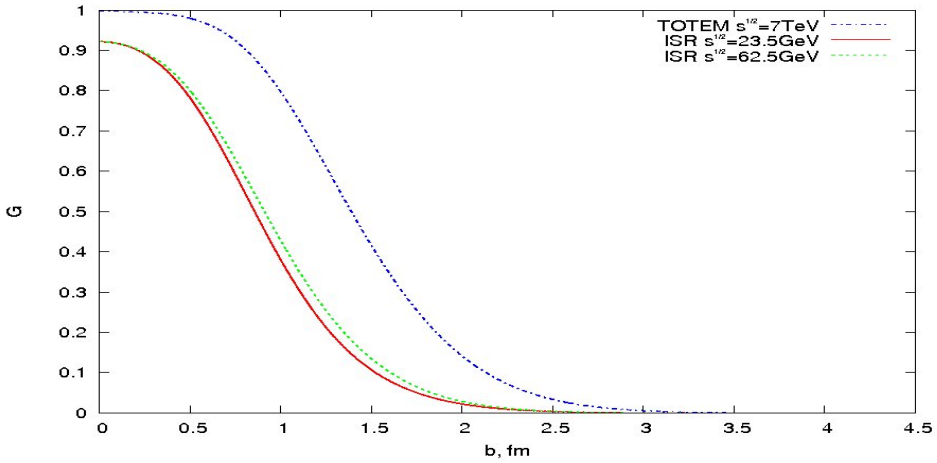

Fig. 3. The overlap functions at 23.5 GeV (solid curve), 62.5 GeV (dotted curve) and 7 TeV (dash-dotted curve).

it approaches the unitarity limit corresponding to the complete blackness. This is a clear manifestation of the parton saturation effect.

The difference between the two functions $\Delta G(b) = G(s_1, b) - G(s_2, b)$ ($\sqrt{s_1} =$ 7 TeV, $\sqrt{s_2} = 23.5$ GeV) results because of the increase of the elastic cross section and shrinkage of the diffraction cone with energy. In other words, it demonstrates the increase of the opacity since the ratio σ_{el}/σ_t increases also, and it is proportional to the opacity.

In Fig. 4, we demonstrate the difference between these two distributions (the upper curve). It is mainly concentrated at the periphery of the proton at the distance about 1 fm. This feature is stable against the variations of ρ_0. It shows that, at higher energies, the peripheral region becomes more populated by partons, and they play more active role in particle production.

It is tempting to ascribe the peripheral nature of this effect to two features of inelastic processes observed already at LHC. First, the collisions with impact parameters about 1 fm lead to the almond-shaped overlap region. Therefore, due to increase of the parton density they become responsible for the ridge-effect visible in high multiplicity pp-processes at LHC but not observed at lower energies. Second, the more peripheral collisions with larger impact parameters would lead to strong increase of the cross section of the inelastic diffraction with large masses and high multiplicities which can hardly be separated by the gap criteria from the minimum bias events. This is especially interesting because the cross section of the low-mass diffraction is rather small at 7 TeV [16] and surprisingly close to its values at ISR energies. The stronger absorption in the peripheral region at

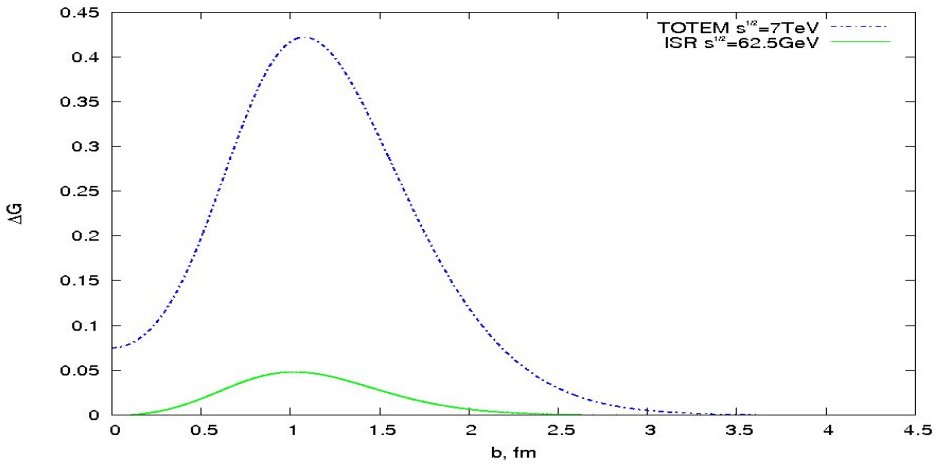

Fig. 4. The difference between the overlap functions. Dash-dotted curve is for 7 TeV and 23.5 GeV energies, solid curve is for 62.5 GeV and 23.5 GeV energies. Conclusion: The parton density at the periphery increases strongly!

7 TeV results in the suppression of the low-mass inelastic diffraction processes. It looks as if it is necessary to include the states of the continuum spectrum beside the discrete bare eigenstates in the traditional approach [17].

We note that the Regge-type models of inelastic diffraction [18] do not agree with the observed decrease below 1 at 7 TeV of the parameter $Z = 4\pi B/\sigma_t$ studied in [8] because they predict that this parameter is equal to $1 + \sigma_{in}^D/\sigma_{el}$ greater than 1 (where σ_{in}^D is the cross section of the low-mass inelastic diffraction). It has been pointed out in [15] that this parameter defines the slope of $d\sigma/dt$ beyond the diffraction cone in the Orear region. Its further decrease with energy would result [19] in first signatures of the approach to the black disk limit to appear just in there.

Another new feature, seen in Fig. 4, is the quite large (about 0.08) value of $\Delta G(b)$ at small impact parameters that reveals a stronger blackness of the disk at higher energies and is related to the rise of the cross section of the main bulk of inelastic processes. No signs of this effect have been found at lower energies. These observations are tightly related to the visible violation of geometric scaling even in the diffraction cone at LHC energies [20] because of the dual correspondence of the transferred momenta t and the impact parameters b. Probably, they correspond also to disagreement between experimental data at 7 TeV and predictions of Monte Carlo models seen in high multiplicity events [21].

In the same Figure, the lower curve corresponds to the similar (albeit

much smaller!) difference $\Delta G(b)$ within the quite narrow ISR energy interval (23.5 - 62.5 GeV). It was stressed in [3] that this difference is negligibly small at low impact parameters while showing some statistically significant excess about 4% at the periphery[2].

Comparison of the curves in Fig. 4 leads to the conclusion that the size of the proton as well as its blackness increase with energy. The protons become more black both in the central region, where they almost reach the saturation of the unitarity condition, and, especially, at the periphery, where the parton density strongly increases. Multiparticle dynamics is in charge of these effects.

References

[1] R. Henzi and P. Valin, Phys. Lett. B **48**, 119 (1974).

[2] F.S. Henyey, R.H. Tuan, and G.L. Kane, Nucl. Phys. B **70**,445 (1974).

[3] U. Amaldi and K.R. Schubert, Nucl. Phys. B **166**, 301 (1980).

[4] U. Amaldi, arXiv:1206.3954.

[5] S. Munier, A.M. Stasto, and A.H. Mueller, Nucl. Phys. B **603**, 427 (2001).

[6] G. Antchev *et al.* (TOTEM Collaboration), Europhys. Lett. **101**, 21004 (2013).

[7] E. Nagy *et al.*, Nucl. Phys. B **150**, 221 (1979).

[8] I.M. Dremin, Physics-Uspekhi **56**, 3 (2013).

[9] C. Bourrely, J.M. Myers, J. Soffer, and T.T. Wu, Phys. Rev. D **85**, 096009 (2012).

[10] D.A. Fagundes, E.G.S. Luna, M.J. Menon, and A.A. Natale, Nucl. Phys. A **886**, 48 (2012).

[11] A.K. Kohara, F. Ferreira, and T. Kodama, Eur. Phys. J. C **73**, 2326 (2013).

[12] A.K. Kohara, F. Ferreira, and T. Kodama, Phys. Rev. D **87**, 054024 (2013).

[13] K. Österberg, talk at EPS-HEP 2013 conference, Stockholm.

[14] I.M. Dremin and V.A. Nechitailo, Phys. Rev. D **85**, 074009 (2012).

[15] I.V. Andreev and I.M. Dremin, ZhETF Pis'ma **6**, 810 (1967).

[16] G. Antchev *et al.* (TOTEM Collaboration), Europhys. Lett. **101**, 21003 (2013).

[17] M.L. Good and W.D. Walker, Phys. Rev. **120**, 1854 (1960).

[18] A.B. Kaidalov, Phys. Rep. **50**, 157 (1979).

[19] I.M. Dremin, Nucl. Phys. A **888**, 1 (2012).

[20] I.M. Dremin, V.A. Nechitailo, Phys. Lett. B **720**, 177 (2013).

[21] S. Chatrchyan *et al.* (CMS Collaboration), Eur. Phys. J. C **73**, 2674 (2013).

[2] This curve differs slightly from that of [3] because we did not use the interpolation procedure adopted there but subtracted directly two overlap functions at 62.5 GeV and 23.5 GeV.